Petroleum Science 19 (2022) 1291–1304

Contents lists available at ScienceDirect

Petroleum Science

journal homepage: www.keaipublishing.com/en/journals/petroleum-science

Original Paper

Research and application of thermal insulation effect of natural gas hydrate freezing corer based on the wireline-coring principle

Yun-Qi Hu [a], Jing Xie [b, *], Shou-Ning Xue [c], Meng Xu [a], Cheng-Hang Fu [b], Hui-Lan He [d], Zhi-Qiang Liu [d], Shao-Ming Ma [e], Si-Qing Sun [e], Chuan-Liu Wang [e]

[a] School of Mechanical Engineering, Sichuan University, Chengdu, 610065, China
[b] MOE Key Laboratory of Deep Underground Science and Engineering, Sichuan University, College of Water Resource and Hydropower, Sichuan University, Chengdu, 610065, China
[c] Zhensha Hydropower Construction Management Branch of Guoneng Dadu River Basin Hydropower Development Co. Ltd, Leshan, 614700, Sichuan, China
[d] Jin Shi Drill Tech Co., Ltd, Tangshan, 063004, Hebei, China
[e] Xi'an Research Institute, China Coal Technology&Engineering Group Corp, Xi'an, 710077, Shaanxi, China

ARTICLE INFO

Article history:
Received 11 July 2021
Accepted 11 October 2021
Available online 24 November 2021

Edited by Xiu-Qiu Peng

Keywords:
Natural gas hydrate
Coring
Cold source freezing
In situ temperature and pressure

ABSTRACT

Natural gas hydrate (NGH) holds great promise as a source of clean energy. It is critical for acquiring the largest possible in situ NGH core for NGH eigen features and resource assessment. However, the existing NGH coring technology has limitations, such as temperature increments, limited coring diameters, low coring rates, and complex coring structures. Therefore, this study designs and proposes an NGH freezing coring (NGHFC) method and verifies the freezing and coring capacities of the NGHFC method in laboratories and experimental wells. Results suggest that NGHFC shows good freezing and heat-retention properties. A freezing core heat transfer model is developed. According to the actual air temperature and operating time, the optimum initial temperature of the cold source can be determined using this model. The average coring rate of NGHFC can reach 77.86%. The research results will provide a new idea of coring gas hydrates.

1. Introduction

Natural gas hydrate (NGH) is also called clathrate hydrates because it looks like ice and shows a cage-like architecture. NGH achieves a high sea area resource density (Liu et al., 2019), and 1 m^3 of NGH can produce 160 m^3 of methane under standard conditions, showing extremely high energy density. The world's NGH reserves were estimated to be 3.02-3.09 $\times$ 10^{18} m^3 (Trofimuk et al., 1973). This result shows that NGH is the clean energy with the greatest development potential in the 21st century, which can solve the energy shortage problem faced by society in the future (Gao et al., 2021a, 2021b, 2021c).

Many scholars have evaluated NGH reserves since their discovery. The predicted reserves of NGH differ owing to differences in evaluation methodologies and measurement accuracy, and the evaluation of NGH reserves decreases each year. Therefore, some experts believe that NGH may not be the primary energy source in the future (Pang et al., 2021). Even the most cautious estimate of NGH reserves is outstanding compared to the total conventional natural gas reserves. Thus, it is essential to evaluate the NGH resource reserves accurately.

The initial stage in determining NGH resource reserves is to conduct deep-sea in situ coring. The coring technique is essential for evaluating NGH reserves, and it also provides critical technological support in allied sectors, such as NGH physical qualities, cold spring ecological inquiry, and deep-sea sediment collection. However, because NGH decomposes when it leaves low temperature, high-pressure environment, it is vital to avoid it from decaying during coring (Wang et al., 2009; Jiang et al., 2015; Xu et al., 2018; Rao et al., 2019; Yoneda et al. 2019a, 2019b), even if the sample is not decomposed. The physical properties will diverge substantially from in situ environments when environmental conditions change greatly (Xie et al., 2021; Gao et al. 2018, 2020). The key to overcoming the relevant research challenges of NGH is to develop a reliable coring method that can reflect the genuine in situ properties of NGH.

* Corresponding author.
E-mail address: xiejing200655@163.com (J. Xie).

https://doi.org/10.1016/j.petsci.2021.11.019

However, many NGH coring devices have been developed and produced using different technologies in various countries. The pressure coring tool with ball valves (PCTB) developed by GEOTEC, UK, pressure core barrel (PCB) adopted by the Deep Sea Drilling Project (DSDP) (Benson et al., 1978; Kvenvolden et al., 1983), advanced piston corer (APC) and pressure core sampler (PCS) used in the Ocean Drilling Program (ODP) (Dickens et al. 1997, 2000; Milkov et al., 2004), Fu-gro pressure corer (FPC) and HY-ACE rotary corer (HRC) used in Hydrate Autoclave Coring Equipment System (HY-ACE) (Amann et al., 1997; Schultheiss et al., 2009), pressure temperature core sampler (PTCS) developed in Japan (Wakishima et al., 1998; Masayuki et al., 2006), multiple autoclave corer (MAC) and dynamic autoclave piston corer (DAPC) used in R.V.SONNE (Hohnberg et al., 2003; Bohrmann et al., 2007; Heeschen et al., 2007), pressure tight piston corer (PTPC) developed by Zhejiang University (Chen et al., 2013; Qin et al., 2016), hole-bottom freezing sampling (HBFS) drilling tool developed by Jilin University (Wang et al., 2015; Sun et al., 2018; Guo et al., 2020), and pressure and temperature preservation system (PTPS) developed by China University of Petroleum (Zhu et al., 2013). Table 1 presents the performance parameters of various technologies and equipment. However, there are some shortcomings of the current gas hydrate-coring device:

(1) During the coring process, pressure stability is insufficient. PCS is the NGH coring tool with the highest pressure sustainability, which can reach about 70 MPa. Pressure preservation is realized by special high-precision technologies, such as rotary ball valve, piston seal at the upper end of the high-pressure chamber, and pressure preservation-coring device seal at the lower end. Pressure compensation is realized by the pressure adjustment compensation system and accumulator. Most of them are sealed by the ball valve, which is easy to get stuck in the coring process. Additionally, it is easy to release pressure in the lifting process due to poor sealing performance, resulting in the decomposition of NGH. The entire corer vibrates greatly in the coring process, and strong mechanical disturbance destroys the truthfulness of in situ stress and pore pressure information.

(2) The temperature and pressure cannot be preserved simultaneously. Except PTCS and HBFS, many coring tools merely offer a thermal insulation layer for heat preservation without cooling measures, which cannot prevent the temperature rise during coring. Thus, they are not temperature-preserved coring. PTCS mainly adopts adiabatic inner tube and thermoelectric inner tube-cooling modes and uses the Peltier effect to maintain hole-bottom temperature by the battery-driven thermoelectric cooling device. The test cannot prove the effectiveness of this device, and this cooling device was canceled in the subsequent improvement. HBFS uses liquid nitrogen or dry ice to freeze the core. However, the extremely low temperature may change the core microstructure, and there is no mechanical structure to form a seal and preserve pressure.

To overcome the shortcomings of the prior art, this study put forward a cold source-based NGH freezing coring (NGHFC) method. The freezing corer's freezing and drilling coring capacities are tested in laboratories and experimental wells. The proposed method adopts a cold source for freezing the NGH core to achieve active heat preservation in the coring process. It also integrates a new pressure preservation controller, which can realize the core's high-pressure sustainability and high-reliability pressure preservation.

2. Introduction of NGHFC structure and coring principle

NGH exists at low temperature and high-pressure environments, and its decomposition depends on four factors: gas composition, condensed phase composition, temperature, and pressure (Koh et al., 2011). Fig. 1 shows the influence of the four factors on the phase state of NGH. The gas composition and condensed phase composition determine the trend of the phase state curve, while the geographical location of NGH determines these two factors. During the coring process, as NGH rises from the seabed to the sea surface, the temperature and pressure changes, causing the NGH state point on the graph to shift to the right and down, and the NGH starts to decompose when it crosses the curve and enters the decomposition region. Therefore, ensuring that the pressure does not drop and the temperature does not rise in the coring process is key for successful coring.

2.1. Temperature and pressure characteristics of NGH

NGH in China is mainly distributed in the nondiagenetic strata within 300 m below the seabed in the southeast ocean area. The representative areas are Qiongdongnan Basin, Xisha Trough, Baiyun Sag in the Pearl River Mouth Basin (including Shenhu sea area), and Okinawa Trough in the East China Sea, according to research data (Zhang et al., 2007; Yuan et al., 2009; Wei et al., 2019; Ning et al., 2020). Table 2 presents the estimated in situ temperature and pressure range of NGH on the seabed.

As shown in Table 2, the in situ temperature range of NGH is 2–24 °C, and the in situ pressure range is 3–28 MPa. The temperature and pressure of NGH in situ are affected by location and depth; therefore, they vary across sea areas. The South China Sea has been identified as a high potential area for one of the world's largest NGH reserves, with the Shenhu sea area having the recent development and potential. Table 3 presents the characteristic parameters of NGH distribution in the Shenhu sea area. The corer

Table 1
Comparison of different NGH coring techniques.

Coring device	R&D institutions	Pressure preservation method	Pressure	Heat preservation method	Coring size	Coring rate
PCTB	GEOTEK Ltd	Ball valve	≤35 MPa	Vacuum insulation	φ51.00 mm × 3.00 m	<50%
PCB	DSDP	Ball valve	≤35 MPa	No heat preservation	φ57.80 mm × 6 m	<15%
PCS	ODP	Ball valve	≤70 MPa	No heat preservation	φ42.00 mm × 0.86 m	14%–76%
FPC	EU- sponsored HYACINTH program	Flip valve	≤25 MPa	No heat preservation	φ50.00 mm × 1.00 m	38%
HRC	EU- sponsored HYACINTH program	Flapper valve	≤25 MPa	No heat preservation	φ51.00 mm × 1.00 m	20%
PTCS	Japan JOGMEC	Ball valve	≤30 MPa	Semiconductor refrigeration	φ66.70 mm × 3.00 m	37%–47%
MAC	the German OMEGA Project	Flapper valve	≤14 MPa	No heat preservation	φ100.00 mm × 0.60 m	–
DAPC	Leibniz Institute of Marine Science	Ball valve	≤20 MPa	No heat preservation	φ84.00 mm × 2.50 m	–
PTPC	Zhejiang University	Flip valve	≤30 MPa	No heat preservation	φ65.00 mm × 0.28 m	–
HBFS	Jilin University	Freezing	–	Cold source	φ50.00 mm × 1.00 m	90%
PTPS	China University of Petroleum, Beijing	Flapper valve	≤30 MPa	Vacuum insulation	φ60.00 mm × 10.00 m	67%

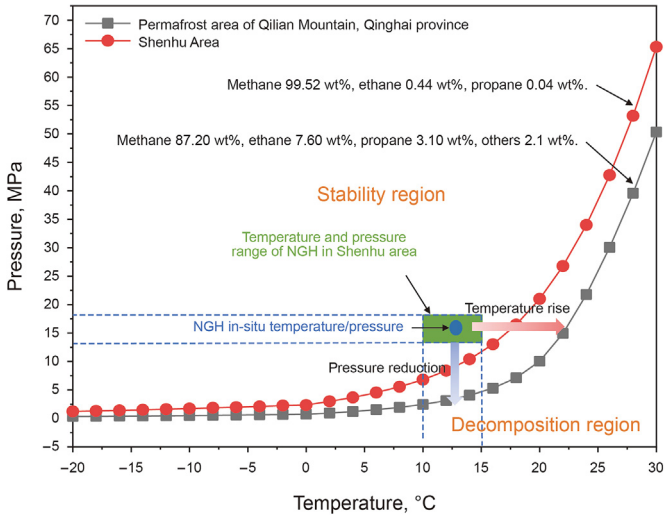

Fig. 1. NGH phase transition curve.

should have a pressure-preserved capacity of at least 20 MPa and a temperature-preserved capacity to keep the core temperature below 15.4 °C during the coring process.

Fig. 1 shows the NGH phase transition curve; if the coring device has no cooling measures, the NGH will decompose due to increased temperature even if the core pressure does not drop. At present, most NGH coring technologies focus on pressure preservation. To slow down the heating rate, only materials with low thermal conductivity are employed. However, to improve the thermal insulation of the corer, a thicker layer of insulation material must be filled, which is contrary to the design requirements of miniaturization and high integration. As the ambient temperature increases, the internal microstructure and pore water pressure of NGH change before reaching the decomposition temperature, which is different from the in situ properties of the formation. To solve this problem, the NGHFC method was proposed. Based on the integrated heat-preserved structure, the core is cooled by the cold source stored in the core, and the NGH state point is moved to the left to increase the decomposition time (the structural schematic diagram is shown in Fig. 2). In the confined space of the corer, the goal of maintaining a relatively stable core temperature and pressure is achieved.

2.2. Wireline coring principle of NGHFC

The wireline-coring principle is a method of obtaining the core without lifting the drill. The NGHFC, which is based on the wireline-coring principle, has the advantage of being easy and quick to use. In continuous coring, NGHFC can enhance efficiency and reduce labor intensity, shown in Fig. 3. As shown in Fig. 4, the coring process of NGHFC is divided into three stages: (a) Corer release, after the external drilling reaches the target horizon, ropes are used to release NGHFC into the drill pipe until the suspension ring make contacts with the drill pipe's inner wall. (b) Drilling and coring, the drill pipe is injected with high-pressure drilling fluid. The internal screw motor generates torque as a result of the drilling fluid, which drives the coring bit to drill. (c) Corer recovery, connect the NGHFC's center rod to the salvage device, and the core pipe will move up over the flap valve and into the freezing tube. The NGHFC can be recovered from the bottom of the hole to the ground and the core inside can be obtained by pulling the salvage device.

2.3. The freezing principle of NGHFC

NGHFC uses multiple low-temperature substances stored in the corer as cold sources to absorb the core heat to achieve the cooling effect; thereby, inhibiting NGH decomposition. The NGHFC structure is designed using the wireline method (Fig. 2). Alcohol is used as the cold source to ensure that the cold source has good low-temperature fluidity. First, use liquid nitrogen to reduce the alcohol to a low temperature and pour the alcohol into the cold source storage chamber. The outer wall of the cold source storage chamber is provided with a thermal insulation layer to prevent the cold source from heating up in advance during the coring process. When NGHFC reaches the NGH formation, high-pressure drilling fluid flows through the screw motor, generating torque and pushing the coring bit down. Stop the drilling fluid circulation when the core has completely entered the core chamber and put the salvage device in place to pull the NGHFC, and the center pole will lift the core chamber to the freezing tube. The flapper valve is closed to preserve pressure, and the cold source absorbs the heat through the wall to freeze the core. Finally, the corer is recovered to obtain the internal frozen pressure-preserved core.

2.4. The pressure-preserved principle of NGHFC

The existing NGH coring technology focuses on maintaining the core's pressure-preserved capacity. At present, the ball and flapper valves are the two main pressure-maintenance structures. The

Table 2
In situ temperature and pressure of each sea area.

Region	In situ temperature	In situ pressure	Depth of NGH stability zone
Qiongdongnan Basin	16 °C–24 °C	21–28 MPa	About 350 m below the sea
Xisha Trough	13 °C–19 °C	13–18 MPa	About 120 m below the sea
Baiyun Sag in the Pearl River Mouth Basin (including Shenhu sea area)	10 °C–24 °C	12–25 MPa	125–355 m below the sea
The northeast slope of the South China Sea (including Taixinan Basin)	8 °C–17 °C	10–17 MPa	110–220 m below the sea
Okinawa Trough in the East China Sea	north: 2 °C–10 °C central: 3 °C –13 °C south: 6 °C–24 °C	north: 3–20 MPa central: 4 –21 MPa south: 5–27 MPa	north: <50 m below the sea central: 25–115 m below the sea south: 90–365 m below the sea

Table 3
Distribution characteristic parameters in Shenhu sea area.

Sea depth	NGH layer depth	NGH layer thickness	In situ temperature	In situ pressure	Stratum lithologic
900–1500 m	100–200 m below the seabed	10–80 m	10.5 °C–15.4 °C	13.8–17.8 MPa	Foraminifera clay silt, silty clay, silt-containing clay

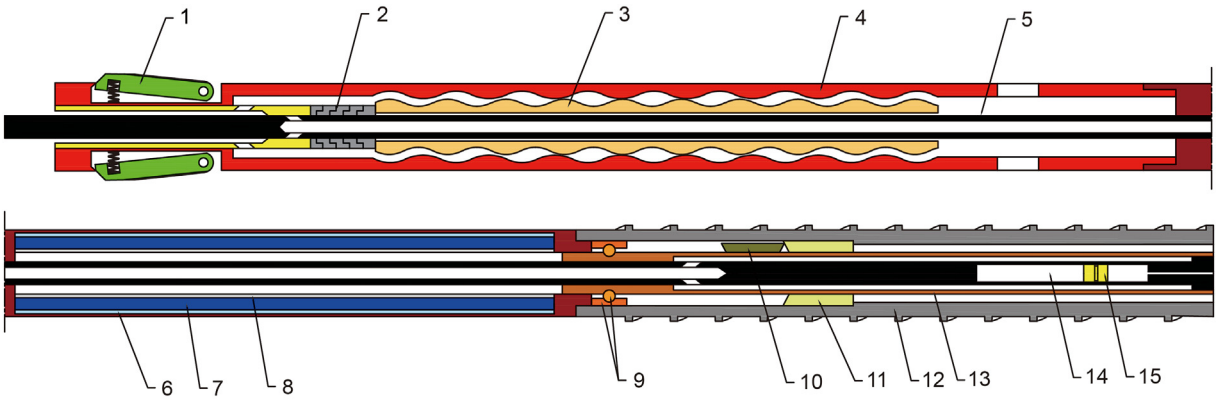

1. spring clip; 2. universal coupling; 3. screw motor; 4. outer tube; 5. center pole; 6. thermal insulating layer; 7. cold source storage chamber; 8. freezing tube; 9. Bearing; 10. flapper valve; 11. valve seat; 12. coring bit; 13. core tube; 14. Accumulator;15. accumulator piston.

Fig. 2. Structure of NGHFC

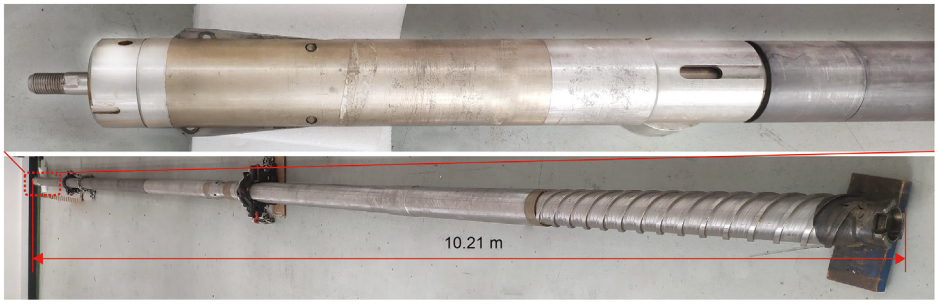

Fig. 3. Physical drawing of NGHFC.

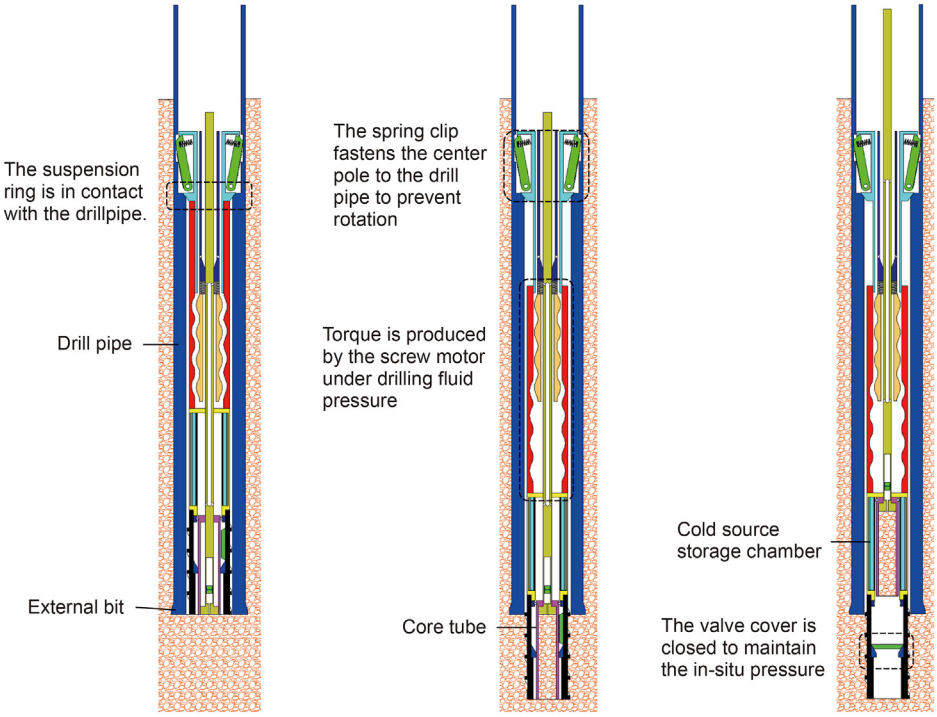

Fig. 4. Schematic diagram of the coring process.

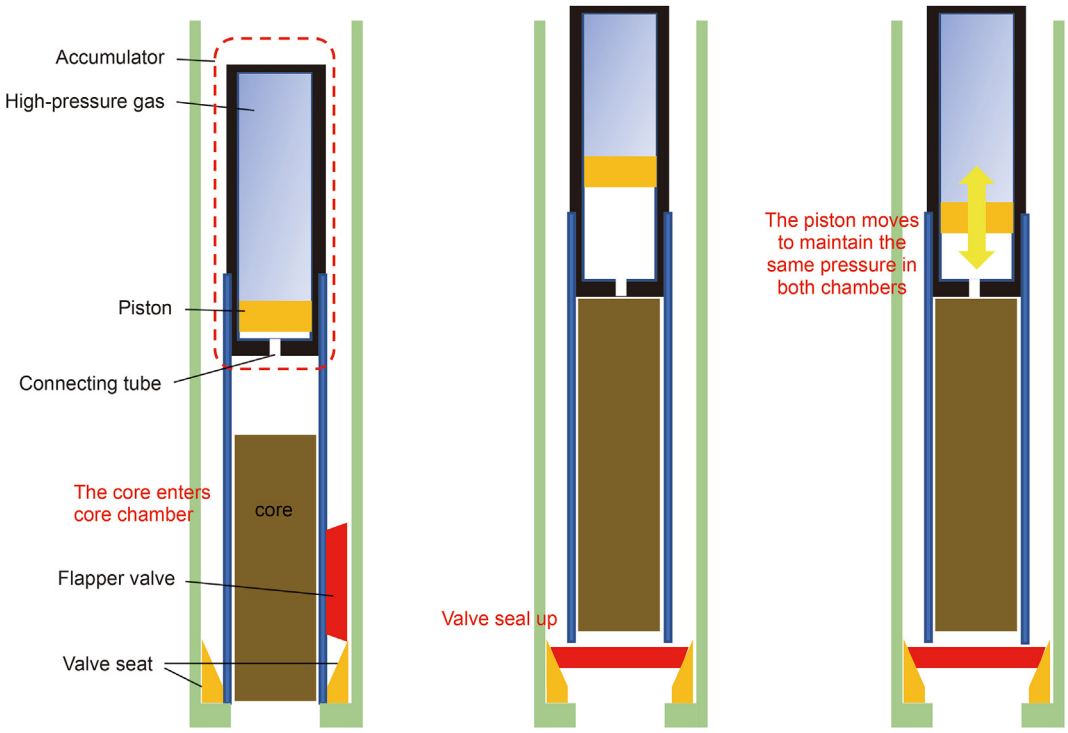

Fig. 5. Working principle of the accumulator.

rotating structure of the flapper valve, as opposed to the ball valve, is less likely to become stuck, making it more suited for large diameter coring (Burger et al., 2003). Furthermore, the closer the sealing surface is to the core tube, the greater the valve cover pressure on the valve seat. Because mechanical vibration is difficult to cause loosening of the sealing surface, the flap valve's sealing effect and vibration resistance are better than the ball valve's. Therefore, NGHFC adopts a flapper valve. NGHFC also integrates an accumulator to compensate for the pressure loss during coring.

Fig. 5 shows the working principle of the accumulator. The upper gas storage chamber of the accumulator is filled with high-pressure gas. The lower part is connected with the core chamber, and a piston connects the two compartments. When the pressure in the core chamber drops during the recovery process of the corer after completing the coring, the piston moves downward to compress the volume of the core chamber, compensate for the

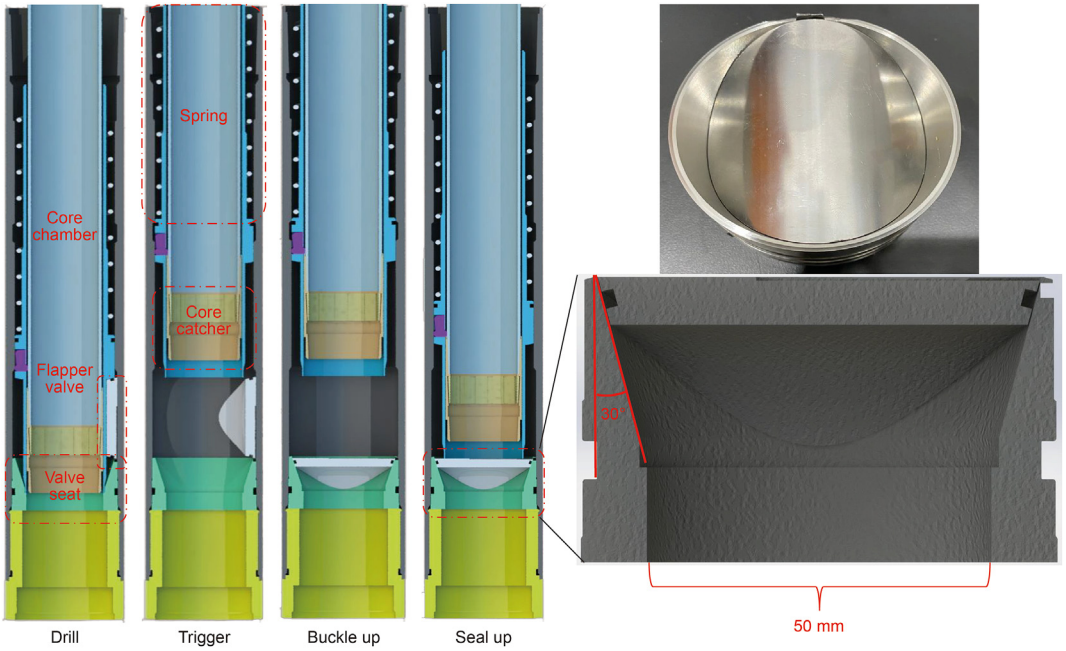

Fig. 6. Operation process of the flapper valve.

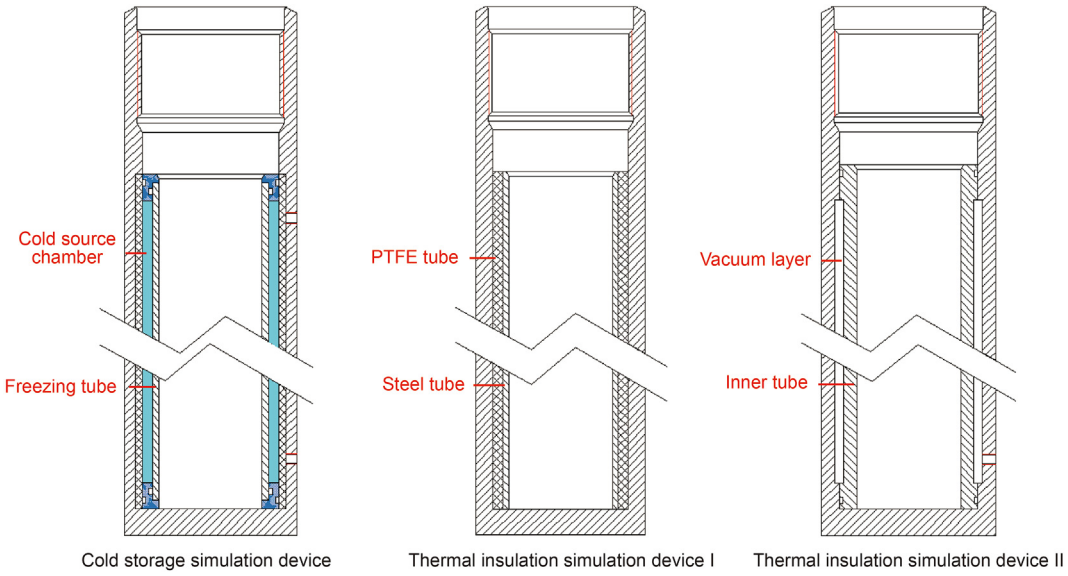

Fig. 7. Schematic diagram of the simulation device.

Table 4
Simulation device parameter.

Device	Inner diameter/outer diameter	Total length/insulation length	Insulation medium
Thermal insulation simulation device I	58.5 mm/98.0 mm	1.22 m/0.94 m	PTFE (thickness: 5.75 mm)
Thermal insulation simulation device II	58.5 mm/98.0 mm	1.22 m/0.94 m	Vacuum layer (thickness: 5.75 mm)
Cold storage simulation device	58.5 mm/98.0 mm	1.22 m/0.94 m	Alcohol (thickness: 5.75 mm, volume: 1.3 L)

Table 5
Comparison of thermophysical properties between simulated and NGH cores.

Parameter	Density, kg/m^3	Specific heat, J/kg·K	Thermal conductivity, W/m·K
Sand with 10 wt% moisture content	1869	1641	1.6
Hydrate core	1985	1362	3.1

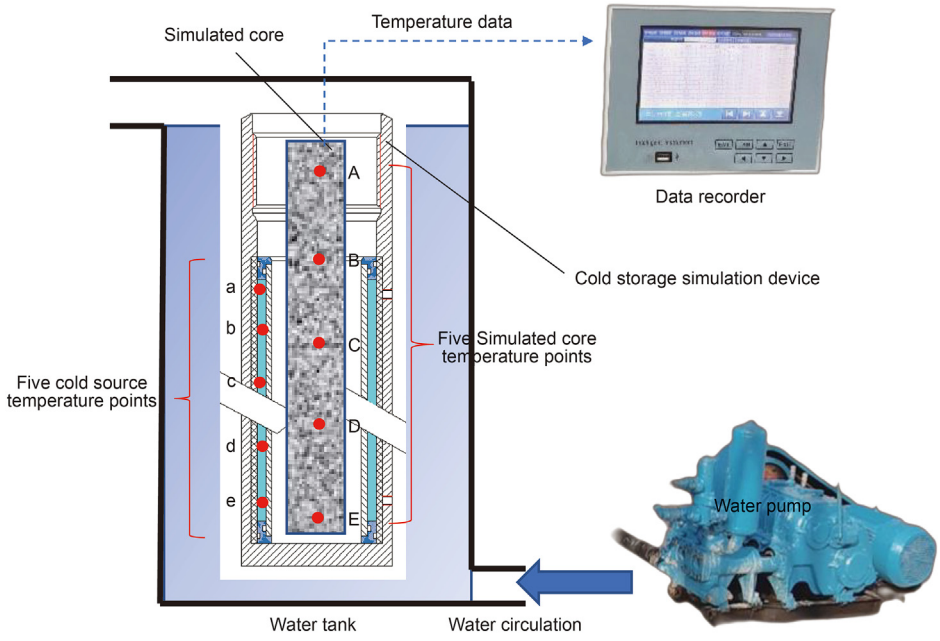

Fig. 8. Schematic diagram of the freezing capacity test system.

pressure loss, and achieve the effect of stabilizing the pressure in the core chamber. The flapper valve adopts Li's A3-type flapper valve designed based on Steinmetz solid structure (Xie et al., 2020; Li et al., 2021).

Fig. 6 shows the structure and movement process. The valve cover flips under the action of the trigger spring to form a seal with the valve seat. Then, the upper spring releases and presses the valve cover to achieve an initial seal. A set of A3-type flapper valves with a sealing surface of 30° conical surface was made of 304 stainless steel. The inner diameter of the valve seat is 50 mm, and the thickness of the valve cover is 8 mm. To test the maximum load-bearing capacity of the flapper valve, the high-pressure container sealed with the A3 flapper valve was continuously pressurized through the hydraulic station. The test results show that the A3-type flap valve can maintain a standard seal under a working pressure of 87.2 MPa, and there is no leakage within 24 h, which can fully meet the needs of deep-sea NGH coring.

3. Experimental test of freezing ability and coring application of NGHFC

To investigate the actual freezing and coring ability of NGHFC, testing is conducted in laboratories and experimental wells, respectively.

3.1. Laboratory freezing ability test

The purpose of the laboratory-freezing ability test is: (1) to compare the difference in the heat preservation effect between the cold source-freezing method adopted by NGHFC and other NGH coring technologies; (2) investigate the temperature changes of internal cold source and simulated core in NGHFC during simulated coring.

(1) Comparison of heat preservation effect between NGHFC and other NGH coring technology.

The existing NGH-coring technology uses low thermal conductivity materials or vacuum layers to reduce heat transfer between cores and the outside world. To compare the difference in thermal insulation performance between the freezing method adopted by NGHFC and the thermal insulation materials, three simulation devices are made according to the internal structure of NGHFC: cold storage simulation device, thermal insulation simulation device I, and thermal insulation simulation device II. The structure of the simulation device is shown in Fig. 7. To imitate the actual heat transfer processes as closely as possible, the dimensions and materials of the cold source storage simulation device are identical to those of the NGHFC. The cold source is put into the cold storage simulation device through the injection port, and polytetrafluoroethylene (PTFE) is employed as a thermal insulation material between the cold source and the outer tube wall. In thermal insulation simulation device I, PTFE is used as a thermal insulation material, and in thermal insulation simulation device II, a vacuum layer is used. The dimensional parameter is a term that refers to the distance between two points. The three simulation devices are shown in Table 4. To simulate the cold source and core heat dissipation process in the actual coring process, sand with 10 wt% moisture content is put into the core tube as the simulated core. Table 5 presents the thermal parameters of the simulated and real NGH cores. The simulated core has a higher specific heat capacity than the real NGH core, indicating that it is more difficult to freeze the simulated core than the real NGH core.

Put the three sets of simulation devices in the refrigerator and cool them to the same temperature. Then, insert the simulated cores with the same initial temperature into the three sets of simulation devices and record the temperature change curves of the three sets of simulated cores with temperature sensors. To enhance the contrast effect, all three groups of simulation devices are cooled to −5 °C. The initial temperature of the simulated core is −5 °C, and the actual in situ temperature of deep-sea NGH will not be lower than 0 °C.

(2) Temperature measurement of NGHFC in simulated coring process

Combined with the cold storage simulation device, water tank, water pump, and simulated core, a set of freezing capacity test systems was developed in the laboratory, and the system component is shown in Fig. 8. In the actual coring process, the coring device needs to be driven by the drilling fluid. In the test system, the water pump is used to pump water into the water tank with a flow rate of 10 m^3/h to simulate the actual coring environment. The test process is divided into three phases (Fig. 9): NGHFC installation, NGHFC coring, and NGHFC core freezing. The heat transfer process of these three phases is simulated by putting the cold storage simulation device in the room temperature air environment, circulating water environment, and putting the cold storage simulation device into the circulating water environment after inserting the simulation core. Three groups of experiments: group I, group II, and group III, were set up as controls. Low-temperature alcohol was used as the cold source at the initial temperature of −50 °C, −75 °C, and −100 °C in the groups and other conditions remained unchanged. Five temperature measuring points were set up in each group of the cold storage simulator and the simulated core. The distance between the two points was 200 mm. They will continuously record the temperature changes of cold sources and cores.

3.2. Core application test

Coring capability is the most basic and important feature that a coring device has. Coring rate (the ratio of actual core length to the feed length of the corer) is a standard parameter used to describe

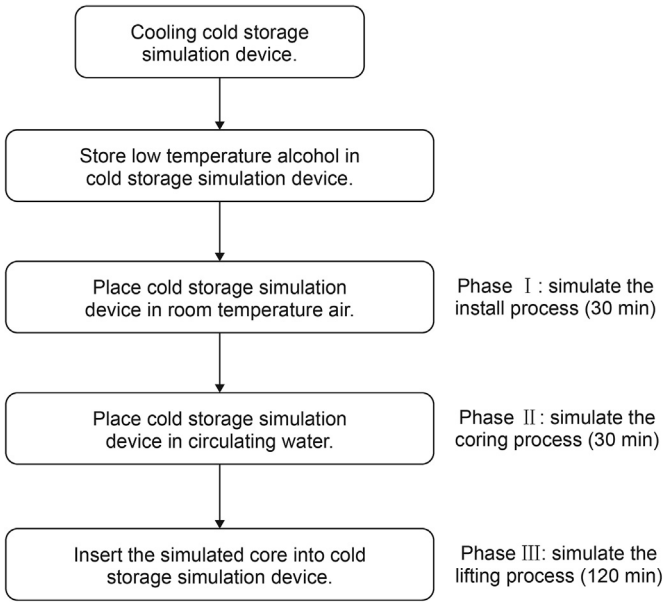

Fig. 9. Test flowchart.

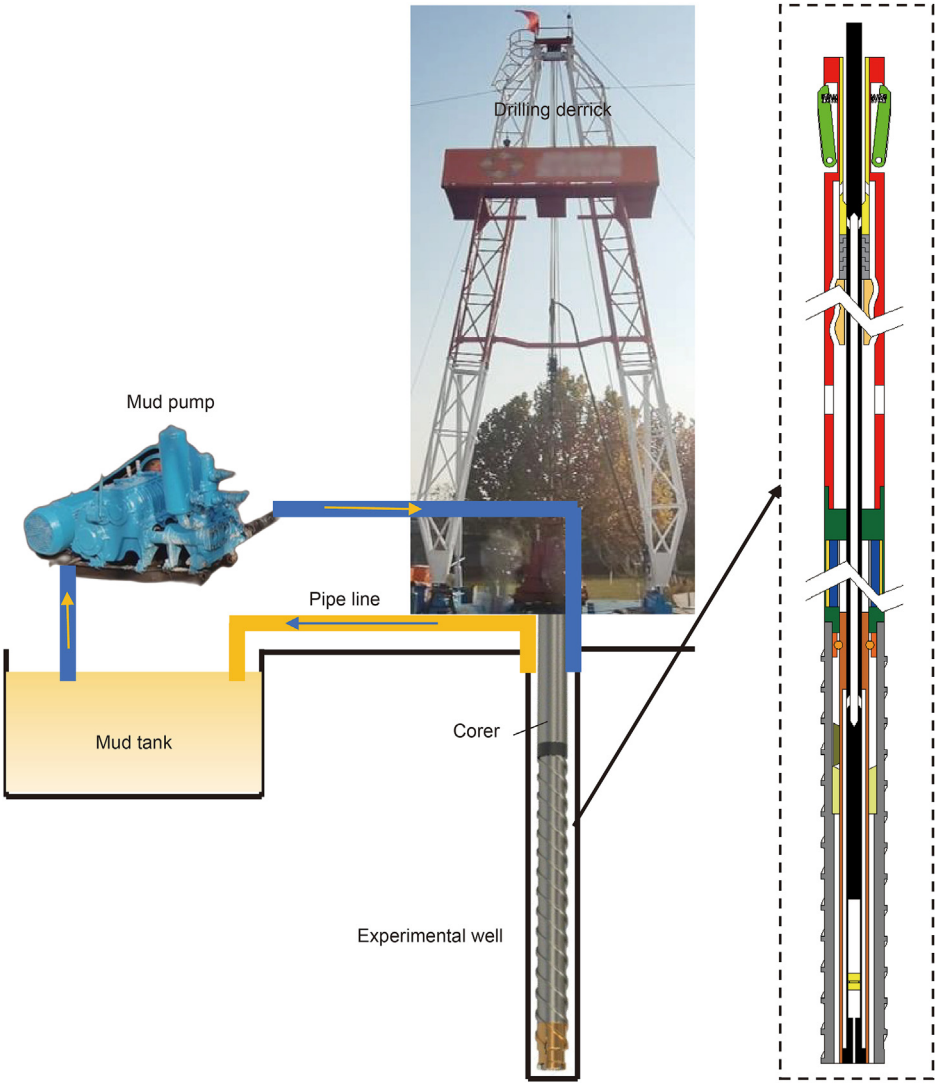

Fig. 10. Coring application test system.

Table 6
Drilling coring parameters.

Parameter	Value
Drilling fluid flow rate	10 m^3/h
Drilling fluid wellhead pressure	1.80 MPa
Coring depth	25–30 m
Coring process time	30 min

Table 7
Core parameters.

No.	Core diameter	Core length	Coring rate	Total coring rate
1	50.00 mm	0.86 m	86%	77.86%
2		0.71 m	71%	
3		0.76 m	76%	
4		0.79 m	79%	

coring capacity, which is determined by a coring test. The coring application test focuses on the coring stability of the NGHFC in the actual downhole working environment.

A coring application test system is developed to test its actual drilling coring ability (Fig. 10). NGHFC was put into the experimental well for the drilling and coring tests. Similar to the freezing ability test, the coring application test is divided into three stages. The operational procedures for each stage are described in section 2.2. Table 6 shows the drilling parameters used in the test. Because of the shallow depth of the well in testing, it takes 30 min for the coring device to release and recover from coring. The actual sea coring depth ranges from 900 to 1500 m; the corer must withstand higher water pressure and work longer. This test is only designed to validate whether NGHFC can obtain a core, because the hole bottom temperature is too different from NGH in situ temperature and the hole bottom space is too small to set a temperature sensor.

NGHFC was subjected to four coring application tests. The core parameters that were obtained during the process are presented in Table 7. Fig. 11 shows the core, which consists of sandstone and clay. The core obtained by NGHFC almost fills the core tube with no visible pile effect. In addition, the core is free of cracks, which is favorable to the microstructure's preservation and can reflect the real formation information. It has an average coring rate of 77.86%. Other NGH coring devices include coring rate of 50% (PTCB) (Benson et al., 1978), 15% (PCB) (Kvenvolden et al., 1983), 14–76% (PCS) (Milkov et al., 2004), 38% (FPC) (Amann et al., 1997), 20%

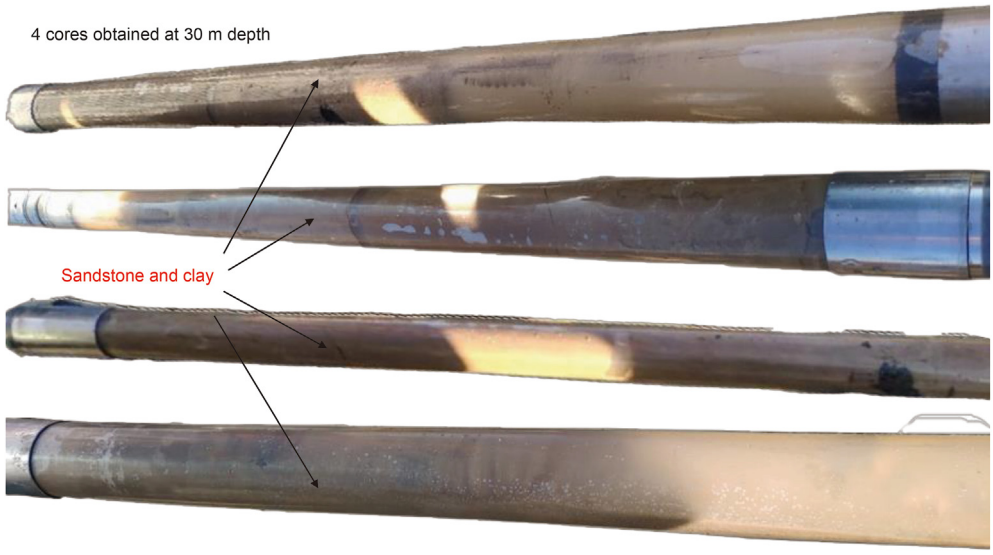

Fig. 11. Four cores obtained in coring application test.

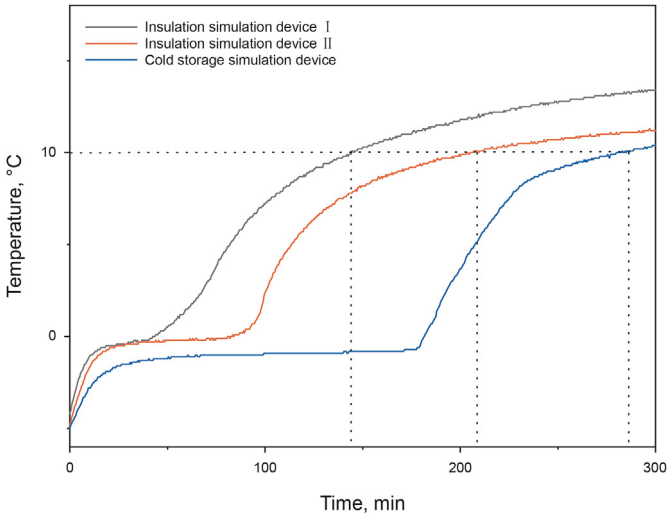

Fig. 12. Comparison of the thermal insulation effect of the PTFE, vacuum layer, and cold source.

(HRC) (Schultheiss et al., 2009), 37–47% (PTCS) (Masayuki et al., 2006), 90% (HBFS) (Wei et al., 2020), and 67% (PTPS) (Zhu et al., 2013). Ranking second among coring technologies above, only 12.14% lower than the HBFS (The core diameter and feed length of FPC and HBFS are identical with those of NGHFC). Drilling fluid with higher viscosity is used in the actual sea area NGH coring process (clear water is used as drilling fluid in the test), which will benefit screw motor driving and core discharge by the drill bit. Therefore, NGHFC may show a better coring effect in the process of NGH coring in real sea areas than in the test. The results showed that NGHFC has a stable coring capacity.

4. Test results and analysis

4.1. Test and analysis of thermal insulation effect

Through the heat transfer experiment of the simulator in the laboratory, the difference in the heat preservation effect between the proposed cold source-freezing method and the existing NGH coring technology is compared. Fig. 12 shows the experimental results. It takes 144, 209, and 280 min for the cores in the thermal insulation simulator I, the thermal insulation simulator II, and the cold storage simulator to rise from −5 °C to 10 °C, respectively. The results showed that in the traditional NGH coring technology, the thermal insulation effect of the vacuum layer is better than that of PTFE. However, the cold source freezing method produces a better thermal insulation effect, and the time spent heating the core from −5 °C to 10 °C is greater than that of the vacuum layer (1.34 times as much as that of the vacuum layer).

The temperature transformation law of the cold source and core (the initial temperature of the simulated core is 5 °C) under different initial temperatures of cold source (the initial temperatures of cold sources in each group are −50 °C, −75 °C, and −100 °C) is tested experimentally. Fig. 13 shows the temperature change curve.

Fig. 13 shows the following results: (1) The lower the cold source initial temperature, the better the freezing effect but it cannot maintain the core's low temperature for an extended time, and the time it takes the core to return to the original temperature in different groups does not change significantly (Fig. 13(b) (d) (f)). It shows that the thermal insulation performance of the device is poor. To prolong the holding time, materials or structures with lower thermal conductivity should be set in corer. (2) The coring stage is the most obvious stage of cold source temperature rise. According to Fig. 13 (a) (c) (e), the average temperature of the three groups of cold sources increased by 34.98 °C, 50.08 °C, and 74.72 °C in the coring stage. The lower the initial temperature, the more obvious the waste of cold energy. (3) The temperature is high at the top and low at the bottom of the core. The lower the temperature of the cold source, the greater the temperature difference between the upper and lower ends of the core. (4) There was no obvious temperature rise of the cold source during the core freezing stage. It can be seen from the above six sets of curves that the core is frozen to the lowest temperature within 5–10 min during the core freezing stage. The lowest temperature of the core is basically consistent with the average temperature of the cold source. (5) The core temperature dropped below 0 °C. However, there was no obvious “plateau period” during the heating process, indicating

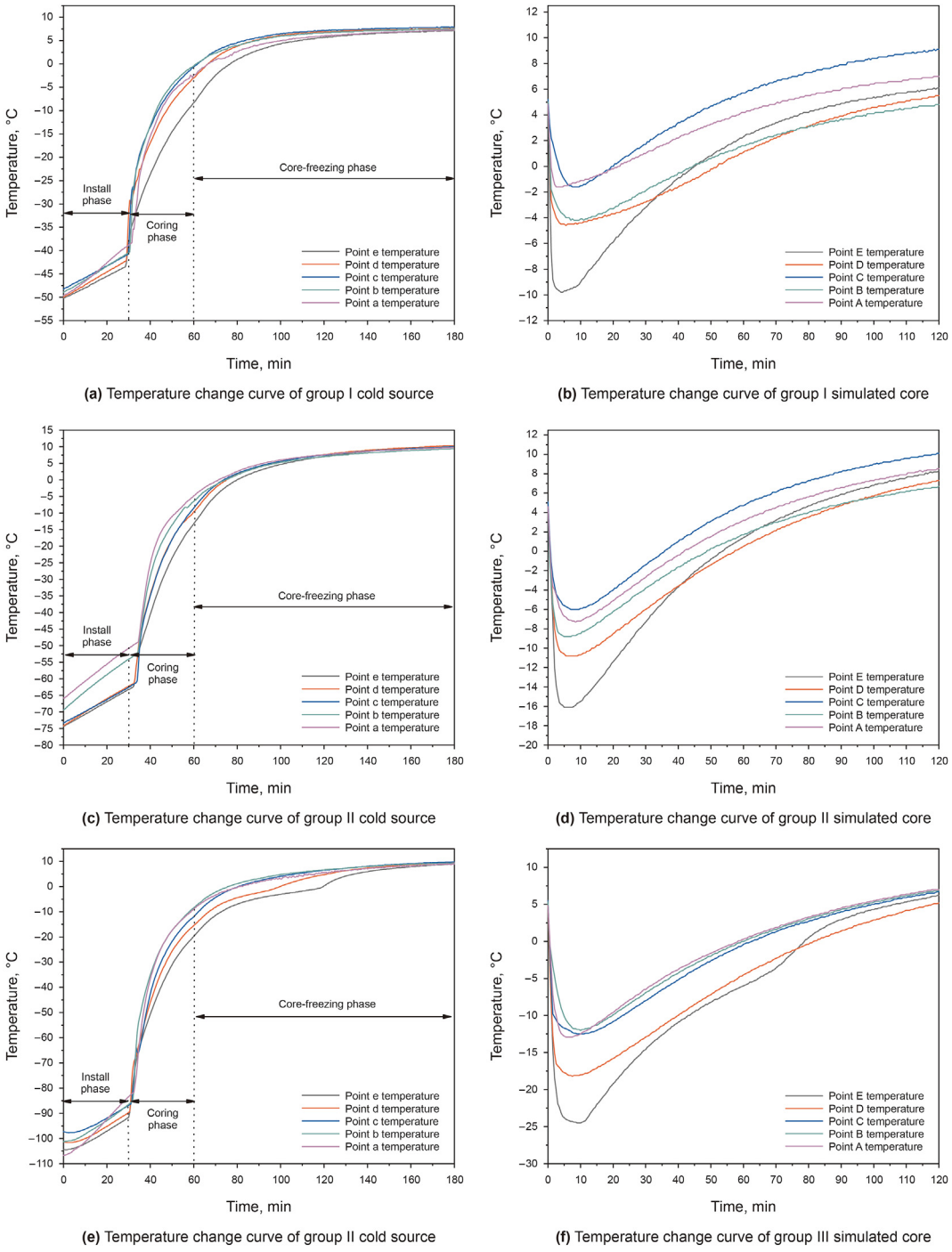

(a) Temperature change curve of group I cold source

(b) Temperature change curve of group I simulated core

(c) Temperature change curve of group II cold source

(d) Temperature change curve of group II simulated core

(e) Temperature change curve of group II cold source

(f) Temperature change curve of group III simulated core

Fig. 13. Temperature change curve of the cold source and simulated core.

that short-term freezing did not cause water crystallization in the core and had little influence on the core microstructure. (6) Currently, it can be ensured that the temperature of the NGH core will not be higher than the in situ temperature within 90 min after leaving the hole bottom (the in situ temperature is assumed to be 5 °C).

4.2. Establishment of temperature-preserved heat transfer model

The room temperature in the laboratory (8 °C–15 °C) is slightly lower than the actual offshore operation; the heat transfer process of the cold source and core is modeled according to the experimental data. Additionally, the influence of environmental and initial temperatures on the cold source and core temperature change is further analyzed. In this study, the heating mechanism of the cold source and core is analyzed from the heat transfer viewpoint.

The heating process of the cold source placed in the annular cavity and the core in the core tube is an unsteady-state heat transfer process. The heat transmission process can be described

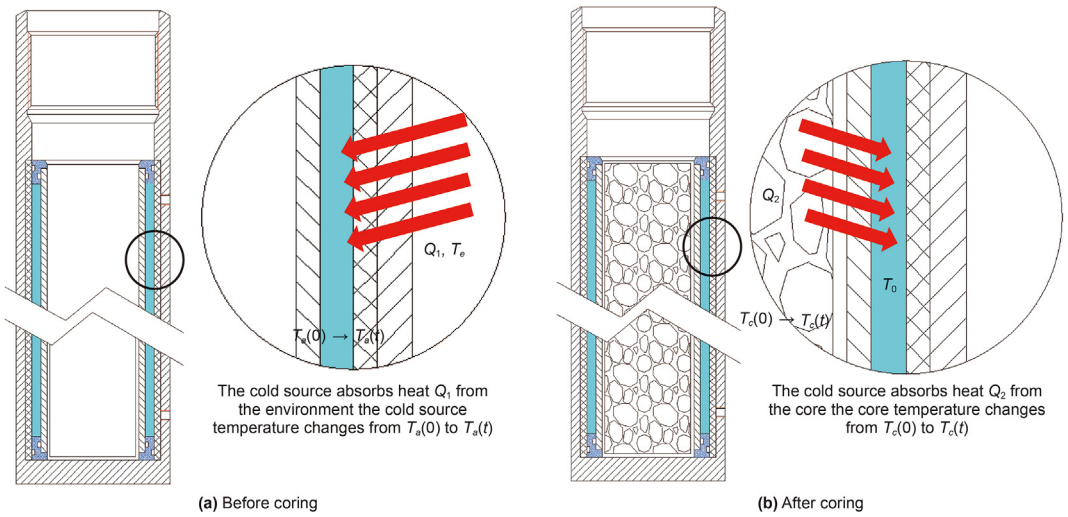

Fig. 14. Schematic diagram of the heat transfer process.

Table 8
Meanings and value of parameters.

Parameters	Meanings	Unit	Value
T_e	Ground ambient temperature	°C	10
T_0	Alcohol temperature at which the core begins to cool	°C	/
m_a	Alcohol mass	kg	1.03
m_c	Simulated core mass	kg	3.67
c_a	Specific heat capacity of alcohol	J/(kg °C)	2230
c_c	Specific heat capacity of the simulated core	J/(kg °C)	1641
R_1	Total thermal resistance of the cold source	K/W	5.812 (in the air) 0.537(in the water)
R_2	Total thermal resistance of the coring system	K/W	0.491

using the lumped parameter method if the internal temperatures of the cold source and the core are the same.

Fig. 14 shows the heat transfer process of the cold source and core. Before the core enters the freezer, it takes $m_a c_a[T_a(t) - T_a(0)]$ J of heat to raise the cold source temperature from $T_a(0)$ to $T_a(t)$. At time dt, the heat absorbed by the cold source from the outside is $dQ = \frac{T_e - T_a(t)}{R_1} dt$. According to the law of conservation of energy, all heat absorbed by the temperature rise of the cold source comes from the external environment; thus, we obtain Eq. (1) as follows.

$$m_a c_a[T_a(t) - T_a(0)] = \int_0^t \frac{T_e - T_a(t)}{R_1} dt \tag{1}$$

We introduce an intermediate variable excess temperature$\theta(t)$.

$$\theta(t) = T_e - T_a(t) \tag{2}$$

Substitute Eq. (2) into Eq. (1) and take the derivative of t:

$$\frac{\frac{d\theta(t)}{dt}}{\theta(t)} = \frac{1}{-mcR} \tag{3}$$

Integral t:

$$\theta(t) = T_e - T_a(t) = e^{-\frac{t}{mcR} + C_1} \tag{4}$$

The variation law of the cold source temperature $T_a(t)$ can be obtained from Eq. (4) and initial condition $\theta(0) = T_e - T_a(0)$.

$$T_a(t) = -e^{\left[-\frac{t}{m_a c_a R_1} + \ln(T_e - T_a(0))\right]} + T_e \tag{5}$$

After the core enters the frozen tube, the cooling process of the core follows the unsteady heat conduction law. Similar to Eq. (5), we can obtain the temperature change law of the core as follows:

$$T_c(t) = -e^{\left[-\frac{t}{m_c c_c R_2} + \ln(T_c(0) - T_0)\right]} + T_0 \tag{6}$$

In Eq. (1) to Eq. (6), $T_a(t)$ represents the temperature of the cold source at time t, $T_c(t)$ represents the temperature of the simulated core at time t. Table 8 presents the meanings and values of the other parameters.

According to Eq. (1) to Eq. (6), the heating process of the cold source in air follows Eq. (7):

$$T_a(t) = (T_a(0) - T_e)e^{-7.491 \times 10^{-5} t} + T_e \tag{7}$$

The heating process of the cold source in circulating water follows Eq. (8):

$$T_a(t) = (T_a(0) - T_e)e^{-8.114 \times 10^{-4} t} + T_e \tag{8}$$

As shown in Fig. 13, the freezing process of the core is extremely fast, and the cooling time is negligible. It is approximate that the core and cold source quickly reach the same temperature. The heating process after the core enters the frozen tube to complete the freezing follows Eq. (9):

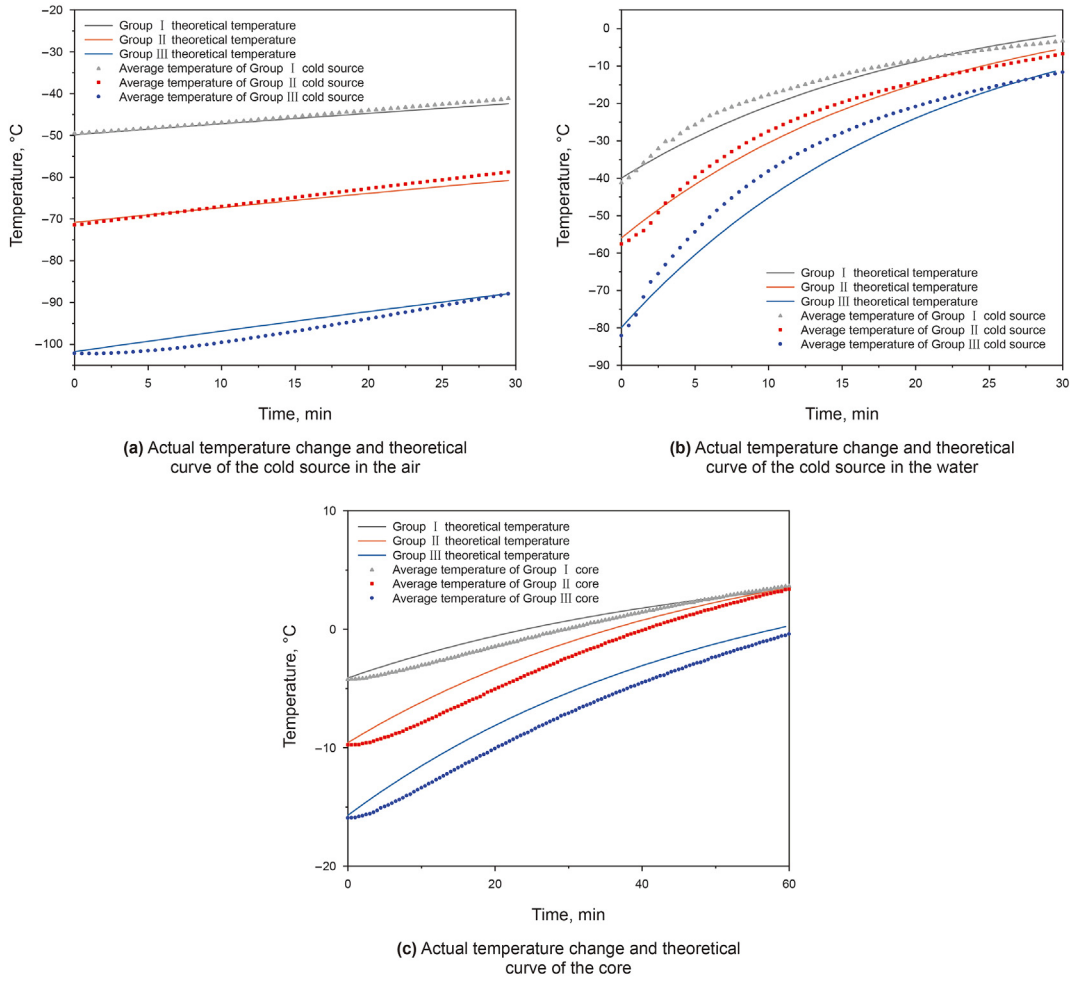

(a) Actual temperature change and theoretical curve of the cold source in the air

(b) Actual temperature change and theoretical curve of the cold source in the water

(c) Actual temperature change and theoretical curve of the core

Fig. 15. Comparison between the actual temperature and theoretical curves.

$$T_c(t) = (T_c(0) - T_e)e^{-3.384\times10^{-4}t} + T_e \tag{9}$$

Here, $T_a(0)$ represent the initial temperature of alcohol and $T_c(0)$ represent the initial temperature of the core.

Another three sets of tests were carried out following the same process (as shown in Fig. 9) to verify the model's accuracy, and three sets of cold source and core temperature data were collected. Fig. 15 shows the actual temperature data and the predicted temperature curve created by the model. It shows that the actual temperature of the core and cold source is consistent with the heat transfer model, which indicates the model is correct.

The cold source and the core temperatures can be predicted according to Eq. (5)-Eq. (6) under any initial temperatures of the cold source and the environment. At the same time, the optimal initial temperature of the cold source can be determined according to the duration of heat preservation.

Assume that the initial temperature of the cold source is T_{a0}, the ambient temperature is T_{e1}, circulating drilling fluid temperature is T_{e2}, the installation stage and coring stage takes time t_1, and t_2 respectively. The temperature law of the core in the freezing stage will follow:

$$T_c(t) = (T' - T_{e2})e^{-\frac{t}{m_c c_c R_2}} + T_{e2} \tag{10}$$

$$T' = \left[(T_{a0} - T_{e1})e^{-\frac{t_1}{c_a m_a R_{1air}}} + T_{e1} - T_{e2}\right]e^{-\frac{t_2}{c_a m_a R_{1water}}} + T_{e2} \tag{11}$$

R_2, R_{1air}, R_{1water} represent the thermal resistance of core, heat transfer resistance of coring device in the air, and heat transfer resistance of coring device in water. According to Eq. (10) Eq. (11), it can be inferred that if the core is to be maintained in t' at a temperature not higher than the original temperature T_{c0}, the optimal initial temperature of the cold source should be lower than T'_{ao}.

$$T'_{a0} = \left[(T_{c0} - T_{e2})e^{\frac{t_2}{c_a m_a R_{1water}} + \frac{t'}{c_c m_c R_2}} + T_{e1} - T_{e2}\right]e^{-\frac{t_1}{c_a m_a R_{1air}}} + T_{e1} \tag{12}$$

5. Summary and prospects

This study proposed an NGH-coring method that simultaneously integrates heat preservation and pressure preservation structure and NGHFC.

To prevent NGH decomposition, NGHFC integrates both pressure preservation and active thermal insulation structures, which are not present in other coring processes. It differs from the semiconductor refrigeration method used by PTCS. NGHFC uses a cold source for refrigeration rather than electricity, which allows less power supply cable structure. The overall integration is higher, and

the radial dimension is lower, making hole bottom operations easier. NGHFC features a pressure preservation structure compared to HBFS, which uses a cold source for refrigeration. The A3-type flap valve used in NGHFC can withstand up to 87.2 MPa for 24 h without leakage.

Furthermore, NGHFC does not require the cold source to completely freeze the core to form an ice valve to achieve pressure preservation, indicating that NGHFC has a smaller cold source consumption. The coring application test results show that the coring rate of NGHFC is greater than that of most existing coring machines. It is proved that the NGHFC is feasible in practical application.

Additionally, this study summarizes the influence of the initial temperature of the cold source and the ambient temperature on the freezing temperature of the core. It establishes the thermodynamic equation during the coring process. The amount of the cold source can be controlled by calculation to prevent the core from being over-frozen to form ice crystals; thereby, destroying its original microstructure. Simultaneously, deep-sea NGH reservoirs are often accompanied by the existence of cold springs. Currently, many scholars are researching the ecology of cold springs. Obtaining live samples of cold spring organisms is the key to cold spring research. NGHFC avoids excessive freezing of the core and can maintain in situ pressure for a long time. It means that the survival rate of microorganisms in the core will significantly increase, which is of great significance for marine biological research and resource development.

It is worth noting that NGHFC will decrease the core temperature during the coring process due to the freezing of cold sources, which is not strictly an in situ temperature-preserved coring. In the future study, we will optimize the heat preservation method to reduce the influence of temperature disturbance on the core's actual in situ properties and morphology.

6. Conclusions

This study develops a cold source-based NGH freezing coring method aiming to solve the problem that NGH is easy to decompose in the coring process. The pressure-preserving and temperature-preserving characteristics of the corer were analyzed, and the average coring ability of NGHFC was evaluated. The main conclusions of this study are as follows:

(1) NGHFC integrates the A3-type flapper valve designed by Li, achieving a pressure-preserved capacity of 86.2 MPa. It can also solve the problem of small coring diameter caused by the ball valve.
(2) Laboratory experiments showed that the cold source-freezing method could actively cool the core during the coring process than the passive heat preservation method with a thermal insulation layer. This can prevent the core temperature from rising rapidly and keep NGH from decomposing for a longer period.
(3) In the laboratory-freezing capacity test, sand with a water content of 10 wt% was used as a simulated core. Low-temperature alcohol with an initial temperature of −100 °C was used as the cold source. After 30 min of installation and 30 min of coring, the core was frozen to −24 °C from an initial temperature of 5 °C, and the temperature was kept below 5 °C for 90 min.

Acknowledgments

The paper was supported by the Program for Guangdong Introducing Innovative and Entrepreneurial Teams (No. 2019ZT08G315), National Natural Science Foundation of China No. 51827901 and U2013603 and Shenzhen Basic Research Project (JCYJ20190808153416970).

References

Amann, H., Hohnberg, H.J., Reinelt, R., 1997. HYACE-a Novel Autoclave Coring Equipment for Systematic Offshore Gashydrate Sampling. Deutsche Wissenschaftliche Gesellschaft für Erdgas und Kohle eV.
Benson, W.E., Sheridan, R.E., 1978. Site 388: lower continental rise hills. Init Rep Deep-Sea Drill Proj 44, 23–68.
Bohrmann, G., Kuhs, W.F., Klapp, S.A., et al., 2007. Appearance and preservation of natural gas hydrate from Hydrate Ridge sampled during ODP Leg 204 drilling. Mar. Geol. 244 (1–4), 1–14. https://doi.org/10.1016/j.margeo.2007.05.003.
Burger, J., Gupta, D., Jacobs, P., et al., 2003. Overview on hydrate coring, handling and analysis. Energy Plan. Pol. Econom. https://doi.org/10.2172/908303.
Chen, J.W., Fan, W., Bingham, B., et al., 2013. A long gravity-piston corer developed for seafloor gas hydrate coring utilizing an in situ pressure-retained method. Energies 6 (7), 3353–3372. https://doi.org/10.3390/en6073353.
Dickens, G.R., Paull, C.K., Wallace, P., 1997. Direct measurement of in situ methane quantities in a large gas-hydrate reservoir. Nature 385 (6615), 426–428. https://doi.org/10.1038/385426a0.
Dickens, G.R., Wallace, P.J., Paull, C.K., et al., 2000. Detection of methane gas hydrate in the pressure core sampler (PCS): volume-pressure-time relations during controlled degassing experiments. Proc. Ocean Drill. Progr. Sci. Results 164, 113–126. https://doi.org/10.2973/odp.proc.sr.164.210.2000.
Gao, M.Z., Zhang, Z.L., Yin, X.G., et al., 2018. The location optimum and permeability-enhancing effect of a low-level shield rock roadway. Rock Mech. Rock Eng. 51 (9), 2935–2948. https://doi.org/10.1007/s00603-018-1461-x.
Gao, M.Z., Zhang, J.G., Li, S.W., et al., 2020. Calculating changes in fractal dimension of surface cracks to quantify how the dynamic loading rate affects rock failure in deep mining. J. Cent. S. Univ. 27 (10), 3013–3024. https://doi.org/10.1007/s11771-020-4525-5.
Gao, M.Z., Xie, J., Guo, J., et al., 2021a. Fractal evolution and connectivity characteristics of mining-induced crack networks in coal masses at different depths. Geomech. Geophys. Geo-Energy Geo-Resour. 7 (1). https://doi.org/10.1007/s40948-020-00207-4. Article Number: 9.
Gao, M.Z., Chen, L., Fan, D., et al., 2021c. Principle and technology of coring with in-situ pressure and gas maintaining in deep coal mine. J. China Coal Soc. 46 (3), 885–897. https://doi.org/10.13225/j.cnki.jccs.YT21.0297.
Gao, M.Z., Xie, J., Gao, Y.N., et al., 2021b. Mechanical behavior of coal under different mining rates: a case study from laboratory experiments to field testing. Int. J. Min. Sci. Technol. 31 (2021), 825–841. https://doi.org/10.1016/j.ijmst.2021.06.007.
Guo, W., Zhang, P.Y., Yang, X., et al., 2020. Development and application of hole-bottom freezing drilling tool for gas-hydrate-bearing sediment sampling. Ocean. Eng. 203. https://doi.org/10.1016/j.oceaneng.2020.107195.
Heeschen, K.U., Haeckel, M., Hohnberg, H.J., et al., 2007. Pressure coring at gas hydrate-bearing sites in the eastern Black Sea off Georgia. Geophys. Res. Abstr. 9.
Hohnberg, H.J., Amann, H., Abegg, F., et al., 2003. Pressurized Coring of Near-Surface Gas-Hydrate Sediments on Hydrate Ridge: the Multiple Autoclave Corer, and First Results from Pressure-Core X-Ray CT Scans. Egs Agu Eug Joint Assembly.
Jiang, M.J., Sun, C., Crosta, G.B., et al., 2015. A study of submarine steep slope failures triggered by thermal dissociation of methane hydrates using a coupled CFD-DEM approach. Eng. Geol. 190, 1–16. https://doi.org/10.1016/j.enggeo.2015.02.007.
Koh, C.A., Sloan, E.D., Sum, A.K., et al., 2011. Fundamentals and applications of gas hydrates. Annu Rev Chem Biomol Eng 2, 237–257. https://doi.org/10.1146/annurev-chembioeng-061010-114152.
Kvenvolden, K.A., Barnard, L.A., Cameron, D.H., 1983. Pressure core barrel: application to the study of gas hydrates. Deep Sea Drilling Project Site 533. https://doi.org/10.2973/dsdp.proc.76.107.1983. Leg 76.
Li, C., Xie, H.P., Gao, M.Z., et al., 2021. Novel designs of pressure controllers to enhance the upper pressure limit for gas-hydrate-bearing sediment sampling. Energy (5), 120405. https://doi.org/10.1016/j.energy.2021.120405.
Liu, L.P., Sun, Z.L., Zhang, L., et al., 2019. Progress in global gas hydrate development and production as a new energy resource. Acta Geol. Sinica - Engl. Ed. 93 (3), 731–755. https://doi.org/10.1111/1755-6724.13876.
Masayuki, K., Satoru, U., Masato, Y., 2006. Pressure temperature core sampler (PTCS). J. Jpn. Assoc. Pet. Technol. 71 (1), 139–147. https://doi.org/10.3720/japt.71.139.
Milkov, A.V., Dickens, G.R., Claypool, G.E., et al., 2004. Co-existence of gas hydrate, free gas, and brine within the regional gas hydrate stability zone at Hydrate Ridge (Oregon margin): evidence from prolonged degassing of a pressurized core. Earth Planet Sci. Lett. 222 (3–4), 829–843. https://doi.org/10.1016/j.epsl.2004.03.028.
Ning, F.L., Liang, J.Q., Wu, N.Y., et al., 2020. Reservoir characteristics of natural gas hydrates in China. Nat. Gas. Ind. 8, 1–24 (in Chinese), CNKI:SUN:TRQG.0.2020-08-002.
Pang, X.Q., Chen, Z.H., Jia, C.Z., et al., 2021. Evaluation and re-understanding of the global natural gas hydrate resources. Petrol. Sci. 18 (2), 323–338. https://doi.org/10.1007/s12182-021-00568-9.

Qin, H.W., Cai, Z., Hu, H.M., et al., 2016. Numerical analysis of gravity coring using coupled eulerian-Lagrangian method and a new corer. Mar. Georesour. Geotechnol. 34 (5), 403–408. https://doi.org/10.1080/1064119X.2014.958880.

Rao, Y.C., Ding, B.Y., Wang, S.L., et al., 2019. Flow pattern and pressure drop of gas-liquid two-phase swirl flow in a horizontal pipe. J. Cent. S. Univ. 26 (9), 2528–2542. https://doi.org/10.1007/s11771-019-4192-6.

Schultheiss, P., Holland, M., Humphrey, G., 2009. Wireline coring and analysis under pressure: recent use and future developments of the HYACINTH system. Sci. Drill. 7. https://doi.org/10.5194/sd-7-44-2009.

Sun, Y.H., Wang, Y., Guo, W., et al., 2018. Hole-bottom freezing technique based on phase change heat transfer for gas-hydrates sampling: efficiency optimization of refrigeration change of phase. Appl. Thermal Eng. Des. Proc. Equipment Econom. 130, 722–734. https://doi.org/10.1016/j.applthermaleng.2017.11.012.

Trofimuk, A.A., Cherskiy, N.V., Tsarev, V.P., 1973. Accumulation of Natural Gases in Hydrate Formation Zones of the World's Oceans. Doklady Akademii nauk SSSR.

Wakishima, R., Imazato, M., Nara, M., et al., 1998. The development of a pressure temperature core sample (PTCS) for the recovery of in-situ methane hydrates. Int Symp Methane Hydrates Proc 107–120.

Wang, Z.Y., Sun, B.J., 2009. Annular multiphase flow behavior during deep water drilling and the effect of hydrate phase transition. Petrol. Sci. 6 (1), 57–63. https://doi.org/10.1007/s12182-009-0010-3.

Wang, Y., Sun, Y.H., Lv, X.S., et al., 2015. Hole-bottom freezing method for gas hydrate sampling. J. Nat. Gas Sci. Eng. 25, 271–283. https://doi.org/10.1016/j.jngse.2015.05.011.

Wei, J.G., Liang, J.Q., Lu, J.G., et al., 2019. Characteristics and dynamics of gas hydrate systems in the northwestern South China Sea - results of the fifth gas hydrate drilling expedition. Mar. Petrol. Geol. 110, 287–298. https://doi.org/10.1016/j.marpetgeo.2019.07.028.

Xie, H.P., Gao, M.Z., Zhang, R., et al., 2020. Study on concept and progress of in situ fidelity coring of deep rocks. Chin. J. Rock Mech. Eng. 39 (5), 865–876. https://doi.org/10.13722/j.cnki.jrme.2020.0138 (in Chinese).

Xie, H.P., Liu, T., Gao, M.Z., et al., 2021. Research on in-situ condition preserved coring and testing systems. Petrol Sci. https://doi.org/10.1016/j.petsci.2021.11.003.

Xu, H.L., Kong, W.Y., Hu, W.G., 2018. Analysis of influencing factors on suction capacity in seabed natural gas hydrate by cutter-suction exploitation. J. Cent. S. Univ. 25 (12), 2883–2895. https://doi.org/10.1007/s11771-018-3960-z.

Yoneda, J., Oshima, M., Kida, M., et al., 2019a. Pressure core based onshore laboratory analysis on mechanical properties of hydrate-bearing sediments recovered during India's National Gas Hydrate Program Expedition (NGHP) 02. Mar. Petrol. Geol. 108, 482–501. https://doi.org/10.1016/j.marpetgeo.2018.09.005.

Yoneda, J., Oshima, M., Kida, M., et al., 2019b. Consolidation and hardening behavior of hydrate-bearing pressure-core sediments recovered from the Krishna–Godavari Basin, offshore India. Mar. Petrol. Geol. 108, 512–523. https://doi.org/10.1016/j.marpetgeo.2018.09.021.

Yuan, Y.S., Zhu, W.L., Mi, L.J., et al., 2009. Uniform geothermal gradient" and heat flow in the qiongdongnan and Pearl River Mouth basins of the south China sea. Mar. Petrol. Geol. 26 (7), 1152–1162. https://doi.org/10.1016/j.marpetgeo.2008.08.008.

Zhang, H.Q., Yang, S.X., Wu, N.Y., et al., 2007. Successful and surprising results for China's first gas hydrate drilling expedition. Fire in the ice. Fall 2007. Methane Hydrate News Lett. 7 (3), 6–9.

Zhu, H.Y., Liu, Q.Y., Wang, G.R., et al., 2013. A pressure and temperature preservation system for gas-hydrate-bearing sediments sampler. Liq. Fuel. Technol. 31 (6), 652–662. https://doi.org/10.1080/10916466.2010.531352.